Self-Assembly and Structure of Interconverting Multinuclear Inorganic Arrays: A $[4 \times 5]$-Ag^{I}_{20} Grid and an Ag^{I}_{10} Quadruple Helicate

Paul N. W. Baxter,[a] Jean-Marie Lehn,*[a] Gerhard Baum,[b] and Dieter Fenske[b]

Abstract: Coordination of the pentatopic ligand **3** with Ag^{I} leads to the simultaneous self-assembly of two polynuclear architectures: a $[4 \times 5]$ grid-type species **10** and a quadruple-helicate **11**, which contain twenty and ten silver ions, respectively. Their structures have been established by X-ray diffraction analysis of the crystals obtained as a mixture on crystallisation. Complex **10** contains two $[2 \times 5]$-Ag^{I}_{10} rectangular subgrids located on opposite sides of an array of parallel ligands of **3** that are twisted into a *transoid* N=C–C=N arrangement around the central C–C bond; it may thus be formulated as a grid of grids: $[2 \times (2 \times 5)]$. Complex **11** is an inorganic quadruple helicate that consists of two sets of two parallel ligands of **3** connected by an array of ten silver ions. Both compounds **10** and **11** are novel types of polynuclear complexes that are composed of two subunits. Their formation points to the possibility of generating specific arrays of metal ions by self-assembly, involving, in particular, a combination of subunits within the overall entity. They represent organised patterns of ion dots of special significance in view of their formal relationship to quantum dots.

Keywords: grid structures · helical structures · multinuclear complexes · N ligands · self-assembly · silver · supramolecular chemistry

Introduction

Discrete molecular entities that lie within the 1 – 100 nm size domain are currently the focus of intense investigations for both scientific and technological reasons. Nanosized molecular structures are expected to display a wealth of novel and intriguing physicochemical properties and open the possibility for the creation of molecular-level devices. The development of new methods for the preparation and study of such entities, which forms part of the emerging fields of nanoscience and nanotechnology, is a subject of paramount importance and is expected to have a major impact on the evolution of materials science in the 21st century.[1, 2]

However, the generation of molecular architectures of nanoscopic dimensions represents a formidable challenge as the time-consuming, sequential bond-formation methodology and usually low overall yields of conventional multistep synthetic techniques may be of limited practical utility for this purpose.

Supramolecular chemistry, on the other hand, offers, in principle, an efficient, economical and direct method of generating nanomolecular architectures, in which the reversible bond formation capacity of self-assembling systems is exploited.[3] This strategy has made successful use of reversible $\pi - \pi$ stacking and solvophobic forces, and H-bonding and metal-ion – ligand coordination interactions for the generation of a wide variety of abiological nanostructures.[3]

The construction of nanostructures that incorporate metal ions is particularly interesting in view of the physicochemical properties and functions that such materials may possess. Supramolecular architectures composed of multiple arrays of metal ions may have, for example, optical, redox, catalytic and magnetic features that are not exhibited by their constituent parts. Through metal-ion-directed self-assembly,[4] it has proven possible to create a large and structurally diverse range of coordination arrays such as helicates,[4a, 5] grids,[6] ladders,[7] cages,[8] circular helicates and rings,[9] rotaxanes,[10] pseudorotaxane racks,[11a–c] and catenanes,[12] in which the metal ions display a high degree of compositional and spatial organisation. In particular, grid-type arrays of electronically communicating metal ions of nanoscopic dimensions could behave as quantum dots and wells and offer, in this respect, exciting prospects for the development of nanosized quantum-confined media.[13]

[a] Prof. Dr. J.-M. Lehn, Dr. P. N. W. Baxter
Laboratoire de Chimie Supramoléculaire
ESA 7006 of the CNRS, ISIS, Université Louis Pasteur
4, rue Blaise Pascal, 67000 Strasbourg (France)
Fax: (+33) 3-88-4110
E-mail: lehn@chimie.u-strasbg.fr

[b] G. Baum, Prof. Dr. D. Fenske
Institut Für Anorganische Chemie der Universität
Engesserstrasse, Geb.-Nr. 30.45
76128 Karlsruhe (Germany)

0947-6539/00/0624-4510 $ 17.50+.50/0

Although most grid-type complexes synthesised to date are nanosized, the tetranuclear [2 × 2] grids fall just within the nanostructural domain,[6c–f] while others display a nuclearity of 6–16 metal ions.[6a,b,g] For the purpose of constructing quantum dots by using such architectures, it is necessary to develop methods for the construction of grids of truly nanometric dimensions and greater metal-ion nuclearity.

As a step towards this goal, we decided to investigate the possibility of preparing a higher order analogue of the previously described [3 × 3] silver grid (**1**),[6a] that is, a [5 × 5] grid (**2**) (Scheme 1). Such a system would represent an ideal starting point as, in analogy to the parent grid **1**, it might form by self-assembly under mild conditions and be readily amenable to solution studies by ^{1}H and ^{109}Ag NMR. An understanding of the factors responsible for the formation of high nuclearity silver grids and subsequent investigations into their physicochemical properties will yield valuable information concerning the feasibility of this approach for the fabrication of supramolecular ion dot and quantum dot arrays.

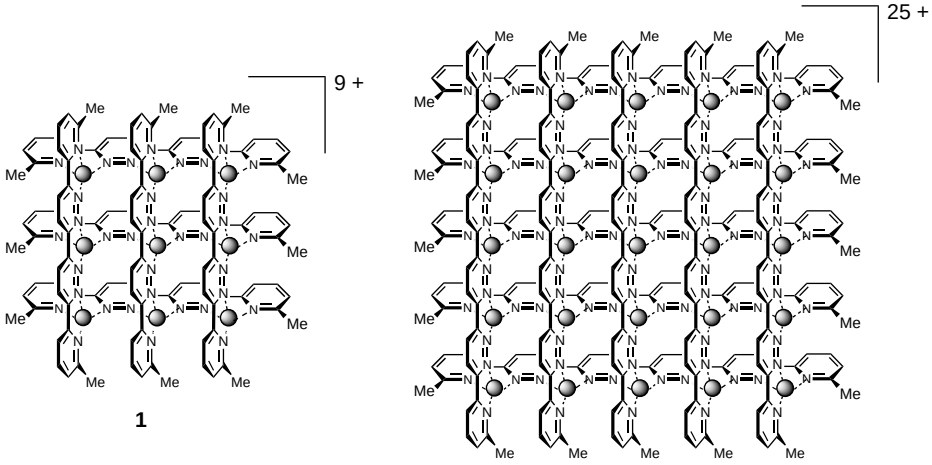

Scheme 1. Schematic representations of the [3 × 3]-Ag^{I}_{9} grid **1**[6a] and a hypothetical larger [5 × 5]-Ag^{I}_{25} analogue **2**; grey spheres = silver(i) ions.

Abstract in French: *La coordination du ligand pentatopique **3** conduit à l'autoassemblage simultané de deux architectures polynucléaires: une entité de type grille [4 × 5], **10**, et un hélicate quadruple **11** contenant respectivement vingt et dix ions Ag^{I}. Leurs structures ont été déterminées par diffraction des rayons X sur les cristaux obtenus en mélange lors de la cristallisation. Le complex **10** contient deux sous-unités de grilles rectangulaires [2 × 5]-Ag^{I}_{10} localisées de part et d'autre d'un ensemble de cinq ligands **3** disposés parallèlement et présentant une conformation N=C–C=N-transoïde autour de la liaison C–C centrale ; il peut ainsi être décrit comme une grille-de-grilles [2 × (2 × 5)]. Le complexe **11** est une hélice quadruple inorganique, un hélicate quadruple, constitué de deux ensembles de deux ligands **3** parallèles, connectés par un réseau de dix ions Ag^{I}. Les deux composés **10** et **11** sont des nouveaux types de complexes polynucléaires formés de deux sous-unités. Leur formation indique qu'il est possible de générer par auto-assemblage des arrangements spécifiques d'ions métalliques, comprenant noamment une répartition en sous-unités au sein de l'entité globale. Ils représentent des réseaux organisés d'ions, des «points ioniques» d'un intérêt particulier du fait de leur rapport aux «points quantiques».*

Results and Discussion

Synthesis of ligand 3: A prerequisite to the generation of structure **2** was the synthesis of the pentatopic decadentate ligand **3** (Scheme 2), which is composed of a central linear array of four pyridazine rings. Oligopyridazines are poorly represented in the literature and high yield synthetic methods for the preparation of compounds possessing more than three rings directly linked in the 3- and 6-positions appear not to have been reported to date.[14] Exploratory synthetic investigations showed that it was possible to prepare ligand **3** by organometallic homoaryl- and heteroaryl-coupling procedures as follows. 2-Chloro-6-methoxypyridazine (**4**) was homocoupled in the presence of a 1:1:4 stoichiometric ratio of zinc, $NiCl_2(H_2O)_4$ and PPh_3 in DMF at 55 °C under argon to give 6,6′-dimethoxy-3,3′-bipyridazine (**5**)[14] in 70% yield after workup. Demethylation of **5** was achieved upon heating at 95 °C in 33% HBr/HOAc for 48 hours. Subsequent removal of solvent under reduced pressure, washing the residue with acetone and neutralisation of a boiling aqueous suspension of the product with aqueous NaOH afforded bis-pyridazone **6**[14c] in near quantitative yield as an insoluble white powder. Bis-pyridazone **6** was converted into 6, 6′-dichloro-3,3′-bipyridazine (**7**)[14c] in 97% yield by heating in $POCl_3$ at 90 °C for 3 hours. Dichloride **7** was then submitted to a statistical Stille heteroaryl coupling with one equivalent of 2-trimethylstannyl-6-methylpyridine (**8**) in the presence of a catalytic amount of $[Pd(PPh_3)_4]$ in toluene at 135 °C for 24 hours.[15a] Chromatographic workup provided 6-(6-methylpyridin-2-yl), 6′-chloro-3,3′-bipyridazine (**9**) in 33–55% yield based upon consumed **7**. Finally **9** was dimerised in DMF at 60 °C by using a 1:1:0.3 stoichiometric ratio of $nBu_4NI/Zn/[NiBr_2(PPh_3)_2]$ as the catalyst.[15b] The target ligand **3** was isolated in 38% yield after workup as a microfibrous khaki solid, insoluble in the standard laboratory organic solvents.

Complexation of ligand 3 with Ag^{+}—NMR spectroscopic investigations: Initial complexation studies revealed that addition of $AgCF_3SO_3$ to nitromethane suspensions of **3** caused rapid dissolution of the ligand over a wide range of **3**/Ag^{+} ratios. This observation highlighted the fact that poor ligand solubility is not necessarily detrimental to successful metal ion binding in view of product solubilisation during self-

  0947-6539/00/0624-4511 $ 17.50+.50/0

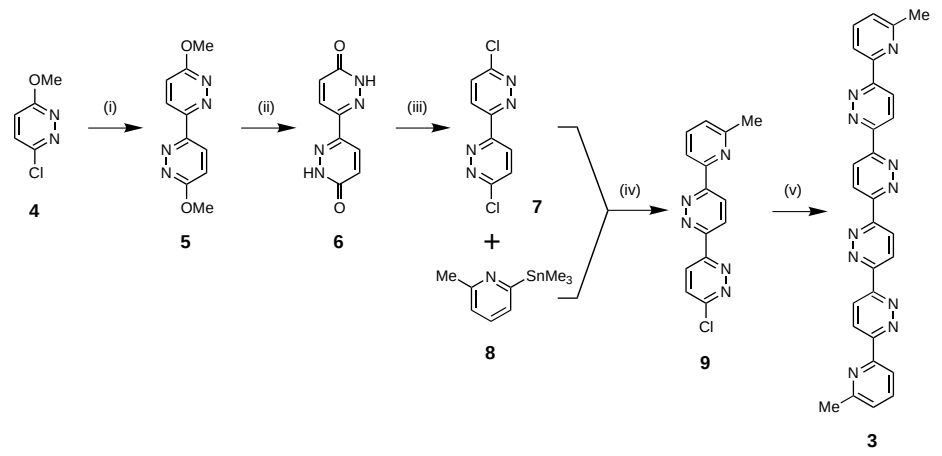

Scheme 2. Synthesis of the linear pentatopic ligand **3:** i) $[NiBr_2(PPh_3)_2]$/Zn/$(n\text{Bu})_4$NI, 60 °C (70 %); ii) 33 % HBr/HOAc, 95 °C (99 %); iii) $POCl_3$, 90 °C (97 %); iv) $[Pd(PPh_3)_4]$, 135 °C, toluene (33–55 %); v) $[NiBr_2(PPh_3)_2]$/Zn/$(n\text{Bu})_4$NI, DMF, 60 °C (38 %).

assembly experiments mediated by metal ions. A ^{1}H NMR titration was therefore performed on reaction solutions of $AgCF_3SO_3$ and **3** in [D_3]nitromethane over a **3**/Ag^+ stoichiometric ratio range from 1:2 to 1:4 in order to obtain a detailed picture of the coordination behaviour of **3** towards Ag^+ ions. At a **3**/Ag^+ ratio of 1:2, a very complex spectrum was obtained indicative of the presence of many slowly exchanging species in solution. Increasing the relative proportion of **3**/Ag^+ to a 1:2.2 ratio caused a dramatic simplification of the spectrum in which the peaks responsible for the original complexity comprised about 20 % of the total resonances present. At a **3**/Ag^+ ratio of 1:2.5, that is, the ratio required to generate the $[5 \times 5]$ grid (**2**), the spectrum consisted of a series of peaks in approximately 2:2:1 ratio that could be interpreted as ligand **3** in three different magnetic environments. The COSY spectrum further reinforced this assignment. For example, the three groups of peaks (each set composed of two doublets and a triplet) corresponding to the protons H3, H4 and H5 of the pyridine rings of **3** were shifted upfield ($\delta = 7.1 - 8.45$) and clearly separated from the pyridazine proton resonances (multiplets at $\delta = 8.74 - 9.24$). The methyl groups gave three strong singlets in a 2:2:1 ratio at $\delta = 2.85$, 2.69 and 2.68, respectively. Further incremental increases in the **3**/Ag^+ ratio to 1:4 caused only minor changes in chemical shift positions and no further apparent alteration in the species distribution.

However, in the NOESY spectrum of the 1:2.5 **3**/Ag^+ reaction solution recorded at 25 °C and −17.5 °C, the H3 and H5 pyridine ring protons of each of the three sets of peaks that correspond to ligand **3** in three different environments, all displayed strong crosspeaks with each other.

Crucial information about the nature of the species present was obtained upon performing a variable temperature proton NMR study on the 1:2.5 **3**/Ag^+ reaction solution (Figure 1). It showed that the ^{1}H NMR spectrum of this solution was composed of two different groups of peaks, one of which is dominant at high temperature, while the other one predominates at low temperature. Thus, heating to 70 °C caused the two doublets and the triplet due to the H3, H5 and H4 protons of the pyridine ring with the original (25 °C) relative integration of one, to increase in intensity to about 95 % of the species present. On the other hand, cooling to −17.5 °C resulted in almost complete disappearance of these last bands and a concomitant increase in intensity of the remaining six resonances that correspond to the H3, H4 and H5 protons of the two environmentally inequivalent ligands of **3** in a 1:1 integration ratio. The spectrum at 25 °C is therefore a superposition of both the low- and high-temperature groups of peaks in a ratio which happens to be about 2:1 at this temperature.

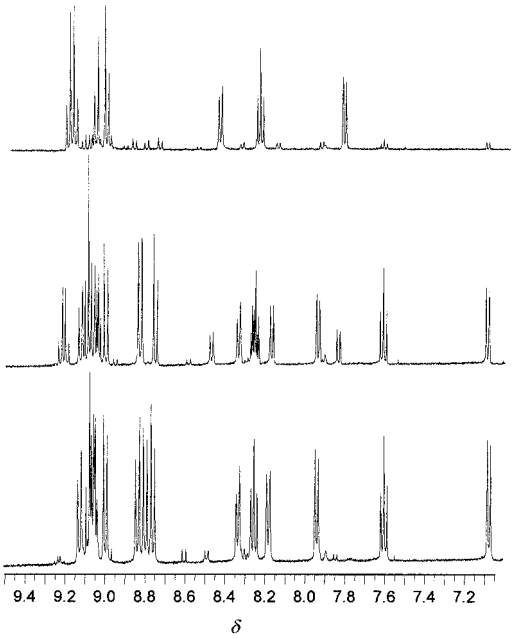

Figure 1. Variable temperature ^{1}H NMR behaviour of the 1:2.5 **3**/Ag^+ reaction solution in [D_3]$MeNO_2$ recorded at 70 °C (top), 25 °C (centre) and −17.5 °C (bottom).

These NMR spectroscopic results allow the following comments to be made.

1) The 1:2.5 **3**/Ag^+ reaction solution consists of an approximately 2:1 mixture of two species that are in slow exchange on the NMR timescale over the temperature range investigated.

2) One of these species (HT) is favoured at high temperature and is almost exclusively present at 70 °C. Its spectrum is that of ligand **3** in a single chemical and magnetic environment and corresponds to a highly symmetric species or to several entities undergoing rapid ligand exchange.

3) Temperature reduction causes progressive conversion into the other species (LT) which is almost exclusively present at −17.5 °C. Its spectrum comprises ligand **3** in two different environments in a 1:1 ratio and shows pyridine proton signals that are markedly shifted upfield with respect to those of HT.

0947-6539/00/0624-4512 $ 17.50+.50/0 *Chem. Eur. J.* **2000**, *6*, No. 24

4) The absence of line broadening and coalescence effects within each spectrum over the whole temperature range indicates that the dominant entities LT and HT, responsible for the low and high temperature spectra, are either single species or pools of complexes exchanging rapidly over the temperature range covered. The observation of crosspeaks between all the ligand signals in the NOESY spectrum can be reconciled with an exchange between the LT and HT entities that is fast with respect to the relaxation-time reference, while being slow on the chemical shift timescale.

5) Anticipating the crystal structure results described below, the LT species could be the quadruple-helicate **11** (Scheme 3, Figure 3 later) which contains four ligands of **3**, each in two different environments, consistent with the NMR spectrum. Of the two sets of pyridine doublet/triplet/doublet proton signals, one is widely spread out and significantly more upfield than the other one. These features are analogous to those observed for the proton NMR spectra of double helicates.[16] Furthermore, the crystal structure below shows that the terminal pyridine ring at one end of one strand is located below the other strand and is therefore shielded with respect to the terminal pyridine ring at the same end of the other strand, which sticks out.

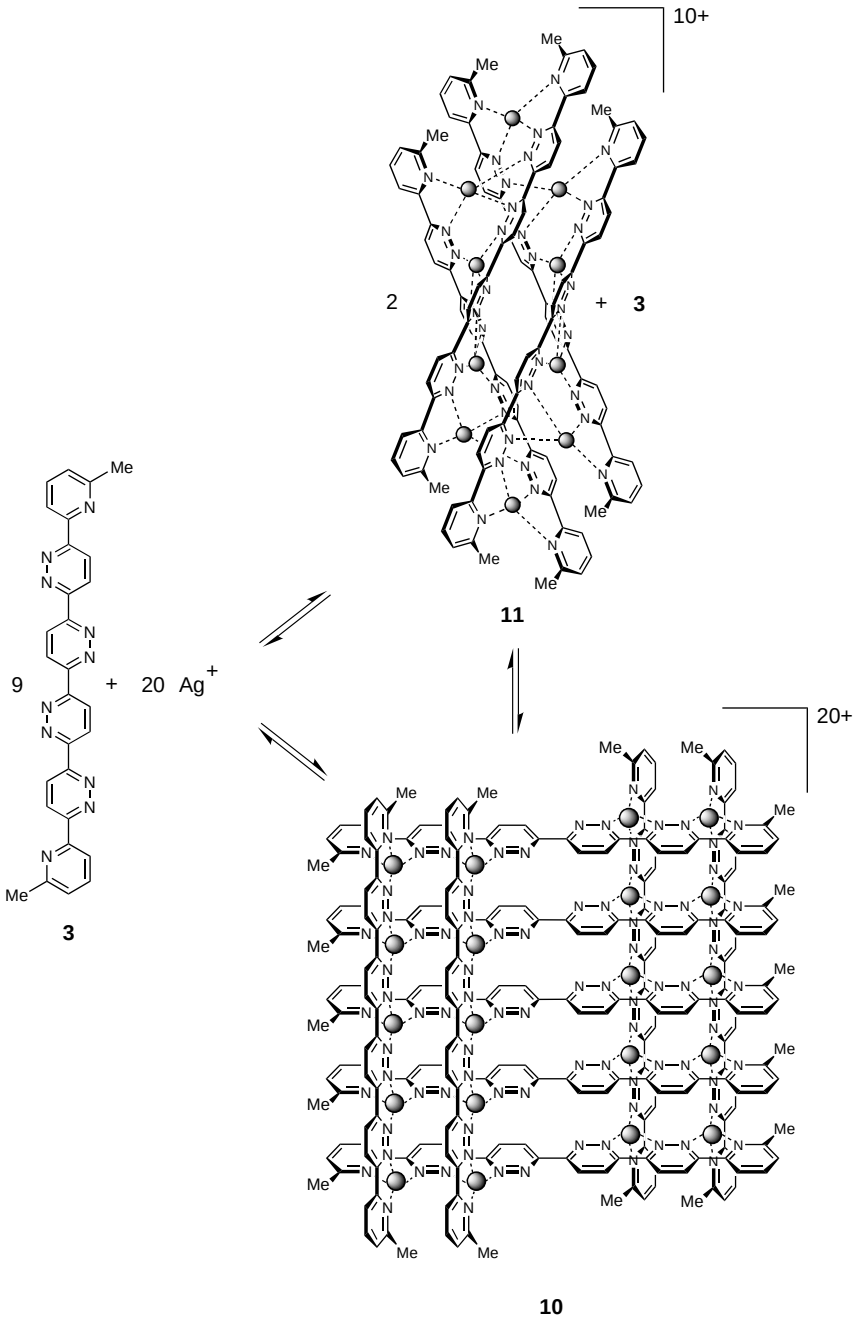

Scheme 3. Schematic representation of the crystallographically characterised icosanuclear [4 × 5] grid **10**-$(CF_3SO_3)_{20}$ and decanuclear quadruple-helical complex **11**-$(CF_3SO_3)_{10}$ and of their self-assembly from the reaction between **3** and $AgCF_3SO_3$ in nitromethane; grey spheres = silver(I) ions.

6) The high-temperature spectrum corresponds either to a HT species of a [2 × 2]-Ag^I_4 grid structure or to a pool of exchanging grid-type or other species. This pool may contain the [4 × 5]-Ag^I_{20} grid characterised below in the solid state, as well as various interwoven forms of [4 × 4]-Ag^I_{16} or [2 × 2]-Ag^I_4 grids.

7) Neither the [4 × 5]-Ag^I_{20} grid **10** (Scheme 3) nor the [5 × 5]-Ag^I_{25} grid **2** are observed in the proton NMR spectrum, at least not in significant amounts as single species. The [5 × 5] grid structure should be disfavoured by the imposition of the *cisoid* form for all ligands, as well as by an overall dome shape for each of a set ligands composed of five units of **3**. The structure **10** contains a set of five ligands in the more stable *transoid* form and is the species that is isolated on crystallisation together with the quadruple-helicate **11**. One may note that **10** can be derived from two species **11** plus one ligand molecule. A more detailed NMR study would be required to gain further information on the nature of the complex processes occuring in solutions of the present sytem.

Solid-state structures of multinuclear Ag^+ complexes of ligand 3

An icosanuclear [4 × 5]-Ag^I_{20} grid-type architecture: Layering a solution of a 1:2.5 ratio of **3**/$AgCF_3SO_3$ in nitromethane with benzene resulted in the development of a mixture of crystals

composed of small, pale-yellow rhombohedra and larger orange blocks. An X-ray crystal structural analysis of the yellow rhombohedra revealed that the constituent cations were indeed that of a high nuclearity Ag^I grid, but not the expected $[5 \times 5]$ grid **2**. The structure instead was that of a strikingly shaped $[4 \times 5]$ grid (**10**) (Figure 2), in which nine ligand **3** components are cemented together by twenty Ag^+ ions. The overall shape of the cation as viewed perpendicularly to its mean plane is that of a distorted rhombohedron of 23.3×23.3 Å including van der Waals radii, which places it well within the nanostructural domain. The nine ligands of **10** are arranged into two sets, the first of which consists of a parallel row of five ligands that are just within van der Waals contact. All ligands within this set are twisted into a *transoid* conformation across the central pyridazine–pyridazine bond so that the middle binding site of each is non-coordinating. Their remaining nitrogens are coordinated to two pairs of silver ions, each of which is situated on opposite edges of each ligand. The second ligand set is composed of four units of **3**, whose nitrogens are all fully coordinated and in a *cisoid* conformation around the central C–C bond. These ligands are arranged into two parallel pairs, which lie on opposite sides of the grid, one above and one below the mean plane through the twenty Ag^+ ions. The ligands within a pair are also just within van der Waals contact. The Ag^+ ions are arranged into two rectangular $[2 \times 5]$ grid-type subsets, which lie on opposite sides of the group of five parallel ligands. The overall array of Ag^+ ions may thus be described as a $[2 \times (2 \times 5)]$-Ag^I_{20} *grid of grids*. The four outer corner Ag^+ ions describe a symmetric rhombus with Ag–Ag separations of 16.699 Å and inner angles of 70° (acute) and 109° (obtuse). Within each column, the average Ag–Ag separation is 3.730 Å along each ligand. The average Ag–Ag distance between the inner Ag^+ of each 2×5 column is 3.928 Å. The average intraligand N-Ag-N

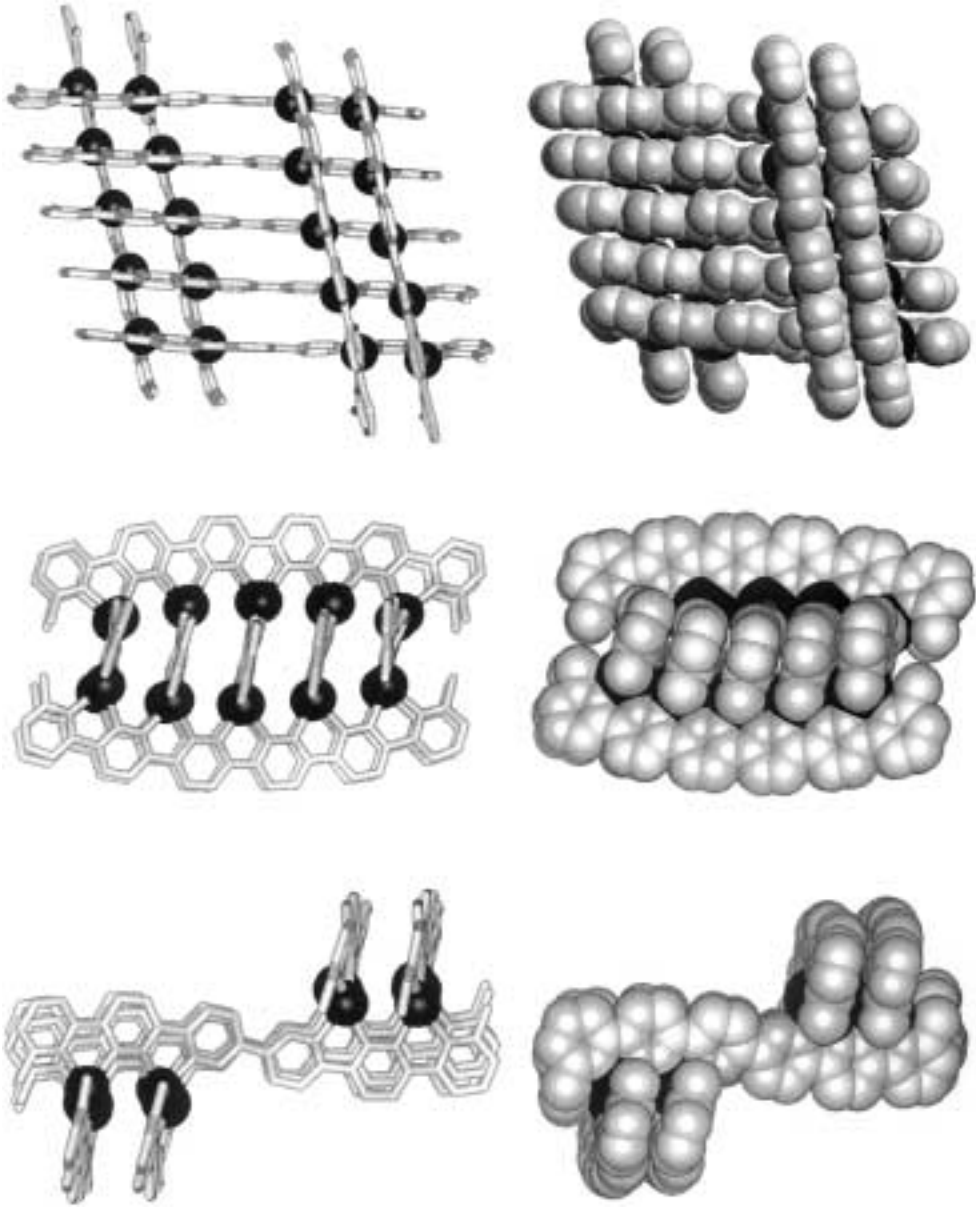

Figure 2. Crystal structure of the icosanuclear $[4 \times 5]$-Ag^I_{20} grid-type architecture **10**: front view (top), side-view along (centre) and perpendicular to (bottom) the array of five parallel ligands; stick (left) and space-filling representations (right); hydrogen atoms are omitted for clarity.

0947-6539/00/0624-4514 $ 17.50+.50/0 *Chem. Eur. J.* **2000**, *6*, No. 24

bond angles are 71.5° for N(py)-Ag-N(pz) and 69.8° for N(pz)-Ag-N(pz) and are unexceptional. The fully coordinated ligands are bent into U-shaped conformations with the concave surface lying on the side of the nitrogens (Figure 2, centre). This results from the fact that the pyridazine rings are not perfect hexagons owing to the shorter N=N bonds. Such a curvature has also been observed in lower nuclearity $[3 \times 3]$- and $[2 \times 3]$-Ag^I grids.[6a,b] The ligands of the set of five parallel units of **3** have a flattened S shape (Figure 2, bottom).

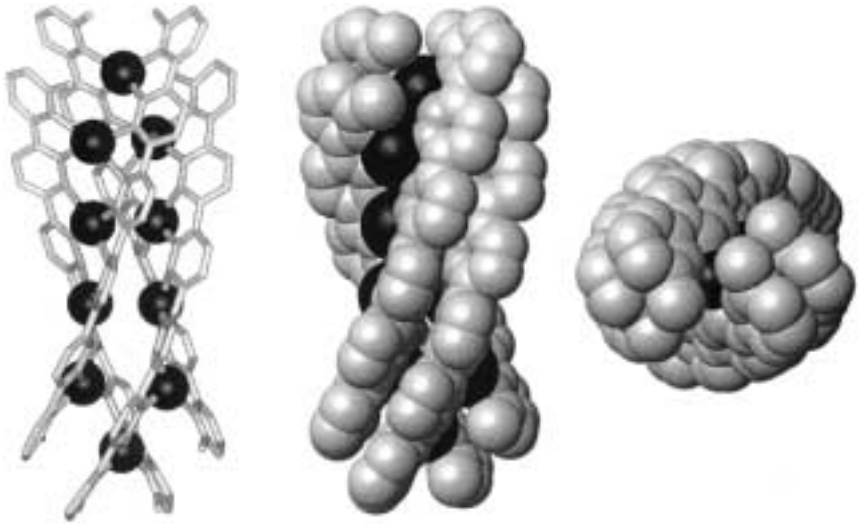

Figure 3. Crystal structure of the quadruple-stranded helicate **11**: perpendicular to (left, centre) and along (right) the axis of the helix; stick (left) and space-filling (centre, right) representations; hydrogen atoms are omitted for clarity.

The reason why the $[5 \times 5]$ grid **2** is apparently not the most stable entity in solution and that the $[4 \times 5]$ grid **10** preferentially forms and crystallises may in part originate from a reluctance to produce a structure that i) has all the ligands **3** in the less stable *cisoid* conformation around the central C–C bond, ii) has a bent, domelike shape in two perpendicular directions (due to the four shorter N=N bonds) and iii) possesses a central Ag^+ ion coordinated by four pyridazine nitrogens, which are poor ligand sites. The averaged Ag–N bond lengths of **10**, $AgPy_2Pyz_2$ (2.32 Å), $AgPyPyz_3$ (2.32 Å) and $AgPyz_4$ (2.40 Å), suggest that the central Ag^+ in **2** would possess particularly long bonds. Both effects may result in a significant destabilisation of **2** relative to **10**. The partially interwoven structure of **10** may therefore represent the best compromise between maximising the number of Ag–N coordination interactions while avoiding five unstable *cisoid* conformations, the poor inner $AgPyz_4$ coordination set and much of the bending effect.

The $[2 \times (2 \times 5)]$ grid-type entity **10** represents an attractive array of silver ions, a set of *ion dots* of well-defined arrangement, and is accessible in one step by self-assembly with formation of 80 $N-Ag^+$ coordinative bonds. One may argue that the grid **10** displays even more interesting features than a fully formed $[5 \times 5]$ square grid **2**, since it possesses two $[2 \times 5]$ rectangular subgrids, which, being located on opposite sides of the mean plane, are in principle accessible separately. Such independent addressing is of much potential value for information handling and switching devices.

A decanuclear Ag^I_{10} quadruple helicate: An X-ray structural determination was also performed on the orange blocks which co-crystallised with **10**-$(CF_3SO_3)_{20}$. It revealed that in this compound, the complex cations were shaped into a quadruple-helical architecture **11** composed of ten Ag^+ ions and four **3** ligands (Figure 3).[16] The Ag^+ ions are arranged into an approximately planar array comprising two parallel and almost linear rows each of four ions, capped top and bottom by the remaining two metals, which are separated by 18.113 Å. In each row the four Ag^+ ions are held in position by two ligands such that the fifth binding site of each ligand **3** lies on opposite sides of the $[Ag_4(\mathbf{3})_2]^{4+}$ unit. The cation **11** may therefore be described as a dimer of two $[Ag_4(\mathbf{3})_2]^{4+}$ units that are connected together by the two capping Ag^+ ions through the terminal, fifth binding site on each ligand. The Ag^+ ions exist in three different highly distorted coordination geometries. The outer two, capping Ag^+ ions possess $Ag(py:pz)_2$ donor sets that appear as partly flattened tetrahedra, and the inner four Ag^+ ions are five-coordinate with distorted trigonal-bipyrimidal Ag(py:pz)(pz:pz) coordination environments. The four centrally positioned Ag^+ ions exhibit distorted five-coordinate square-based pyramidal and flattened tetrahedral coordination polyhedra with variable occupancy. The fifth site of each of the five-coordinate Ag^+ ions is ligated by a water molecule. Each inner pair of Ag^+ ions of the two $[Ag_4(\mathbf{3})_2]^{4+}$ units are separated by an average of 3.396 Å, which is greater than the sum of their van der Waals radii (2.52 Å for Ag^+).[17] The quadruple strand is composed of two subsets: two pairs of ligands wrapped around the axis of the helix. The overall structure of **11** may therefore be described as a $^4H[\{2 \times (\mathbf{3})_2\}\text{-}Ag^I_{10}]$ helicate (Figure 3). Each ligand **3** has two different halves; it is highly distorted and twisted into a propellor-blade-type conformation about its long axis. Triflate anions, nitromethane and water solvent molecules fill the interstices between the complex cations **11**.

Conclusion

In conclusion, the successful generation, isolation and characterisation of two high nuclearity species, a $[4 \times 5]$-Ag^I_{20} silver grid **10** of nanometer size and a quadruple Ag^I_{10} helicate **11**, has been achieved upon reaction of $AgCF_3SO_3$ with the pentatopic ligand **3**. The formation of **10** amounts to the establishment of 80 Ag^+-N coordination interactions! The products can be isolated from an equilibrating mixture of complexes in solution, whose speciation profile varies with temperature. In terms of programmed self-assembly,[3a] the

formation of the [4 × 5] grid **10** rather than of the [5 × 5] grid **2** underlines the obvious fact that, despite the strength of the coordination interactions/instructions and of the resulting trend towards maximal site occupation, other factors, such as structural strain, stacking, environmental effects and so on may interfere and influence the nature of the thermodynamically (or also kinetically) favoured output entity. All these contributions play a role and the robustness of a given directing code depends on the balance between them.

The overall structure of both species **10** and **11** may be described as being composed of two substructures, a [4 × 5] grid of two [2 × 5] grids, $[2 \times (2 \times 5)]$-Ag^{I}_{20}, for **10** and a quadruple strand of two double strands, $^{4}H[\{2 \times (\mathbf{3})_2\}$-$Ag^{I}_{10}]$, for **11**. The formation of **10** and **11**, therefore, amounts to the self-assembly of seggregated subsets within a global architecture.

The simultaneous formation and interconversion of **10** and **11** in solution adds a flavour of dynamic diversity, which is of interest within the framework of dynamic combinatorial chemistry.[19]

The present results demonstrate the feasibility of generating high-nuclearity, internally structured, inorganic ion-dot arrays of nanometric size, by using metal-ion-mediated self-assembly, and opens the way to the creation of a wide variety of entities with quantum-confined properties. These arrays present, in particular, intriguing relationships to metal-based quantum-dot cells[18], extending such devices into the multi-dot domain with self-generation ability, while by-passing the recourse to sophisticated and demanding nanofabrication techniques. Further studies are currently directed towards the design, exploitation and development of nanosized inorganic supramolecular architectures based on spontaneous but controlled self-assembly processes.

Experimental Section

General: ^{1}H (500 MHz) and ^{13}C (125.8 MHz) NMR spectra were recorded on a Bruker ARX500 spectrometer and were referenced to the residual protonated solvent in the deuterated solvent. The NMR spectra of **3** were referenced to added Me_4Si. The ^{1}H NMR of **3** was unambiguously assigned on the basis of COSY and ROESY measurements. The reaction solutions used in the ^{1}H NMR titration experiments were each prepared in the following way: the appropriate volume of a 3.23×10^{-2} mol dm^{-3} stock solution of $AgCF_3SO_3$ in $[D_3]MeNO_2$ was added to **3** (2.0 mg) in an NMR tube by microsyringe and the mixture made up to a 1 mL volume with $[D_3]MeNO_2$. The solutions were then briefly ultrasonicated to disperse the solid and incubated at 70 °C for 48 h to give clear yellow solutions that were used subsequently for NMR measurements. The solutions were surprisingly insensitive to light and could be stored for many months without decomposition.

6-(6-Methylpyridin-2-yl)-6′-chloro-3,3′-bipyridazine (9): Toluene (38 mL) was added by syringe to **7**[14c] (0.279 g, 1.23×10^{-3} mol), **8**[20] (0.314 g, 1.23×10^{-3} mol) and $[Pd(PPh_3)_4]$ (0.056 g, 4.85×10^{-5} mol) under an argon atmosphere, and the stirred solution heated in an oil bath at 135 °C for 36 h. All solvent was then distilled off under reduced pressure, and the residue was purified by chromatography on a column of alumina (Merck, standard activity II/III), eluting first with CH_2Cl_2 to recover unreacted **7** (0.042 g), and then with 3 % MeCN/CH_2Cl_2 to obtain the desired product. After removal of solvent on a water bath, the remaining solid was suspended in Et_2O (5 mL) briefly stirred, filtered under vacuum, washed with Et_2O (4 mL) and air-dried to give **9** (0.164 g, 35–55 % based upon reacted **7**) as pale yellow needles. ^{1}H NMR ($CDCl_3$, 500 MHz, 25 °C): $\delta =$ 8.858 (d, $J_{5,4} = 8.9$ Hz, 1H; inner pyridazine H5), 8.846 (d, $J_{4',5'} = 8.9$ Hz, 1H; chloropyridazine H4′), 8.788 (d, $J_{4,5} = 8.9$ Hz, 1H; inner pyridazine H4), 8.521 (d, $J_{3,4} = 7.8$ Hz, 1H; pyridine H3), 7.793 (t, $J_{4,3;4,5} = 7.7$ Hz, 1H; pyridine H4), 7.713 (d, $J_{5',4'} = 8.9$ Hz, 1H; chloropyridazine H5′), 7.279 (d, $J_{5,4} = 7.7$ Hz, 1H; pyridine H5), 2.654 (s, 3H; Me); ^{13}C NMR ($CDCl_3$, 125.8 MHz, 25 °C): $\delta = 159.6$, 158.6, 157.8, 155.8, 155.0, 152.2, 137.4, 129.0, 127.0, 125.6, 125.3, 124.7, 118.8, 24.6 (Me); EIMS: m/z (%): 283 (100) $[M]^+$, 255 (79) $[M - N_2]^+$, 220 (55) $[M - N_2 - Cl]^+$, 192 (62) $[M - 2N_2 - Cl]^+$; elemental analysis calcd (%) for $C_{14}H_{10}ClN_5$: C 59.27, H 3.55, N 24.68; found C 59.42, H 3.32, N 24.57.

6,6‴-Bis-(6-methyl-pyridin-2-yl)-[3,3′:6′,6″:3″,3‴]quaterpyridazine (3): Anhydrous DMF (8 mL) was added by syringe to nBu_4NI (0.766 g, 2.07×10^{-3} mol), zinc dust (0.135 g, 2.07×10^{-3} mol) and $NiBr_2(PPh_3)_2$ (0.500 g, 6.73×10^{-4} mol) under an argon atmosphere in a dried schlenk tube, and the mixture was stirred at 30 °C for 2 h, after which time it had turned dark brown. Anhydrous DMF (20 mL) was added by syringe to a separate dried, argon-filled schlenk that contained **9** (0.588 g, 2.07×10^{-3} mol), and the suspension was heated until all the solid had dissolved. After cooling for some minutes to about 80 °C, the nickel catalyst solution was added through a cannula, and the resulting black mixture placed in a bath at 60 °C and stirred at this temperature for 48 h. The mixture was then poured onto saturated aqueous Na_2EDTA (200 mL) and stirred for a further 24 h. The pale brown suspension was isolated by filtration under vacuum, washed with excess distilled water and dried in air. The solid was then suspended in MeOH (30 mL), briefly ultrasonicated, filtered under vacuum, washed with excess MeOH and air-dried. Further purification was achieved upon boiling the solid in $CHCl_3$, isolation by filtration under vacuum and washing the filter cake with hot $CHCl_3$ until the collected filtrate was colourless. Compound **3** thus obtained (0.246 g, 38 %) after additional air-drying appeared as a pale khaki fibrous solid. ^{1}H NMR (CF_3COOD, 500 MHz, 25 °C): $\delta = 9.599$ (d, $J_{4',5'} = 9.0$ Hz, 2H; inner pyridazine H4′), 9.555 (d, $J_{5',4'} = 9.0$ Hz, 2H; inner pyridazine H5′), 9.254 (d, $J_{4,5} = 9.1$ Hz, 2H; outer pyridazine H4), 8.962 (d, $J_{5,4} = 9.1$ Hz, 2H; outer pyridazine H5), 8.802 (t, $J_{4,3;4,5} = 8.0$ Hz, 2H; pyridine H4), 8.747 (d, $J_{3,4} =$ 8.0 Hz, 2H; pyridine H3), 8.194 (d, $J_{5,4} = 8.0$ Hz, 2H; pyridine H5), 3.21 (s, 6H; Me); all chemical shifts of **3** represent a magnetically and chemically equivalent pair of protons, only one of each pair is numbered in the assignment above; ^{13}C NMR (CF_3COOD, 125.8 MHz, 25 °C): $\delta = 160.2$, 158.6, 156.7, 155.9, 153.5, 150.4, 146.3, 134.8, 134.7, 132.6, 131.5, 130.1, 125.4, 21.3 (Me); FAB$^+$ MS (CF_3COOH): m/z (%); 497 (100) $[M+1]^+$; FAB$^+$ HRMS calcd m/z for $[M+1]^+$: 497.19388; found 497.19373.

Preparation of silver complexes—representative example: $MeNO_2$ (2 mL) was added to a mixture of **3** (0.0150 g, 3.0×10^{-5} mol) and $AgCF_3SO_3$ (0.0194 g, 7.55×10^{-5} mol) and the reaction was briefly ultrasonicated, then stirred in a bath at 70° C for 48 h. The orange solution was filtered by gravity, and the solvent removed under vacuum to yield 0.034 g (99 %) of an orange solid, which was composed of **10**, **11** and possibly additional entities. This solid could subsequently be redissolved in nitromethane for ^{1}H NMR studies and crystallisations.

Crystal data for $[Ag_{20}(\mathbf{3})_9][(CF_3SO_3)_{20}]$ (10-$(CF_3SO_3)_{20}$): Small, pale yellow rhombohedra suitable for measurement were grown by slow diffusion of benzene into a solution of a 1:2.5 ratio of **3**/$AgCF_3SO_3$ in nitromethane. X-ray data: $(C_{252}H_{180}N_{90}Ag_{20}) \cdot 2(C_6H_6) \cdot (C_6H_{14}) \cdot 3(CH_3NO_2) \cdot 4(CH_3OH) \cdot 20(CF_3SO_3)$; STOE-IPDS diffractometer with a graphite monochromatised $Mo_{K\alpha}$ radiation ($\lambda = 0.71071$ Å). φ scans, at 173 K. The unit cell was triclinic with a space group of $P\bar{1}$. Cell dimensions: $a = 18.828(4)$ Å, $b =$ 21.708(4) Å, $c = 28.361(6)$ Å, $\alpha = 110.81(3)°$, $\beta = 107.64(3)°$, $\gamma = 90.17(3)°$, $V = 10246(4)$ Å^3 and $Z = 2$ ($M_w = 8807.49$, $\rho = 2.855$ g cm^{-3}). Structure solution and refinement: structure solution by direct methods and refined (based on F^2 with all independent data) by full-matrix least-square methods (SHELXTL 97). The data was corrected for Lorentz and polarisation factors; no absorption correction was applied. Hydrogen atoms were included at calculated positions by using a riding model. Reflections were collected from $2.0° \le \theta \le 24.98°$ for a total of 41732 reflections of which 20501 were unique ($R_{int} = 0.038$) with $I > 4\sigma(I)$; number of parameters = 2251. Final R factors were $R1 = 0.093$ (based on observed data), w$R2 = 0.276$ (based on all data), GOF = 1.882, maximal residual electron density = 1.521 e Å^{-3}. Excess electron density is present and could not be associated to any particular part of the molecule or solvent molecules. Also, five of the counterions are either incomplete or could not be located on the electron difference map; this is presumably due to a weak

0947-6539/00/0624-4516 $ 17.50+.50/0 *Chem. Eur. J.* **2000**, *6*, No. 24

data collection and partly associated to such a large void within the crystal lattice.

Crystal data for $[Ag_{10}(3)_4](CF_3SO_3)_{10}$ (11-$(CF_3SO_3)_{10}$): Orange blocks selected for measurement co-crystallised along with the pale yellow rhombohedra from the 1:2.5 **3**/$AgCF_3SO_3$ crystallisation solution described above. X-ray data: $C_{112}H_{80}N_{40}Ag_{10}\cdot(OH^-)\cdot 5.5(H_2O)\cdot 1.75(C_6H_6)\cdot 9(CF_3SO_3)\cdot 5(CH_3NO_2)$; STOE-IPDS diffractometer with a graphite monochromatised $Mo_{K\alpha}$ radiation ($\lambda = 0.71071$ Å). φ scans, at 173 K. The unit cell was orthorhombic with a space group of *Pbcn*. Cell dimensions: $a = 75.380(15)$ Å, $b = 31.430(6)$ Å, $c = 24.590(5)$ Å, $\alpha = \beta = \gamma = 90^\circ$, $V = 58258(20)$ Å^3 and $Z = 4$ ($M_w = 4967.45$, $\rho = 0.566$ g cm^{-3}). Structure solution and refinement: structure solution by direct methods and refined (based on F^2 by using all independent data) by full-matrix least-square methods (SHELXTL 97). The data was corrected for Lorentz and polarisation factors; no absorption correction was applied. Hydrogen atoms were included at calculated positions by using a riding model. Reflections were collected from $1.8^\circ \le \theta \le 21.01^\circ$ for a total of 29479 reflections of which 17860 were unique ($R_{int} = 0.089$) with $I > 4\sigma(I)$; number of parameters = 2653. Final R factors were $R1 = 0.1516$ (based on observed data, w$R2$ = 0.3838 (based on all data), GOF = 1.499, maximal residual electron density = 2.070 e Å^{-3}. Crystallographic data (excluding structure factors) for the structures reported in this paper have been deposited with the Cambridge Crystallographic Data Centre as supplementary publication no. CCDC-145033 (quadruple-helicate **11**) and 145034 (grid **10**). Copies of the data can be obtained free of charge on application to CCDC, 12 Union Road, Cambridge CB2 1EZ, UK (fax: (+44) 1223-336-033; e-mail: deposit@ccdc.cam.ac.uk).

Acknowledgement

We thank Dr. R. Khoury for his contribution to the refinment of the crystal structures and R. Graf for some of the NMR measurements.

[1] a) A. J. Baird, *Integrated Chemical Systems: A Chemical Approach to Nanotechnology*, Wiley Interscience, NY, **1994**; b) G. A. Ozin, *Adv. Mater.* **1992**, *4*, 612.

[2] For some recent examples, see for instance: a) A. Globus, C. W. Bauschlicher, Jr., J. Han, R. L. Jaffe, C. Levit, D. Srivastava, *Nanotechnology* **1998**, *9*, 192; b) J. K. Gimzewski, C. Joachim, *Science* **1999**, *283*, 1683; c) C. Mao, W. Sun, Z. Shen, N. C. Seeman, *Nature* **1999**, *397*, 144; d) U. B. Sleytr, P. Messner, D. Pum, M. Sára, *Angew. Chem.* **1999**, *111*, 1034; *Angew. Chem. Int. Ed.* **1999**, *38*, 1034.

[3] a) J-M. Lehn, *Supramolecular Chemistry: Concepts and Perspectives*, VCH, Weinheim, **1995**, Chapter 9, pp. 139–197; b) D. Philp, J. F. Stoddart, *Angew. Chem.* **1996**, *108*, 1242; *Angew. Chem. Int. Ed. Engl.* **1996**, *35*, 1154.

[4] For recent reviews on metal ion-mediated self-assembly, see for example; a) P. N. W. Baxter in *Comprehensive*, *Supramolecular Chemistry*, *Vol. 9* (Eds.: J. L. Atwood, J. E. D. Davies, D. D. MacNicol, F.Vögtle, J.-M. Lehn), Pergamon, Oxford, **1996**, Chapter 5, pp. 165–211; E. C. Constable in *Comprehensive*, *Supramolecular Chemistry*, *Vol. 9* (Eds.: J. L. Atwood, J. E. D. Davies, D. D. MacNicol, F.Vögtle, J.-M. Lehn), Pergamon, Oxford, **1996**, Chapter 6, pp. 213–252; M. Fujita in *Comprehensive*, *Supramolecular Chemistry*, *Vol. 9* (Eds.: J. L. Atwood, J. E. D. Davies, D. D. MacNicol, F.Vögtle, J.-M. Lehn), Pergamon, Oxford, **1996**, Chapter 7, pp. 253–282; b) R. F. Saalfrank, *Curr. Opin. Solid State Mat. Sci.* **1998**, *3*, 407; c) B. Olenyuk, A. Fechtenkotter, P. J. Stang, *J. Chem. Soc. Dalton Trans.* **1998**, *11*, 1707; d) M. Fujita, *Polym. Mater. Sci. Eng.* **1999**, *80*, 27; e) D. L. Caulder, K. N. Raymond, *J. Chem. Soc. Dalton Trans.* **1999**, *8*, 1185; f) C. Piguet, *J. Inclusion Phenom. Macrocyclic Chem.* **1999**, *34*, 361; g) S. Leininger, B. Olenyuk, P. J. Stang, *Chem. Rev.* **2000**, *100*, 853.

[5] a) C. Piguet, G. Bernardinelli, G. Hopfgartner, *Chem. Rev.* **1997**, *97*, 2005; b) M. Scherer, D. L. Caulder, D. W. Johnson, K. N. Raymond, *Angew. Chem.* **1999**, *111*, 1690; *Angew. Chem. Int. Ed.* **1999**, *38*, 1588.

[6] a) P. N. W. Baxter, J.-M. Lehn, J. Fischer, M.-T. Youinou, *Angew. Chem.* **1994**, *106*, 2432; *Angew. Chem. Int. Ed. Engl.* **1994**, *33*, 2284; b) P. N. W. Baxter, J.-M. Lehn, B. O. Kneisel, D. Fenske, *Angew. Chem.* **1997**, *109*, 2067; *Angew. Chem. Int. Ed. Engl.* **1997**, *36*, 1978; c) P. N. W. Baxter, J.-M. Lehn, B. O. Kneisel, D. Fenske, *Chem. Commun.* **1997**, 2231; d) G. S. Hanan, D. Volkmer, U. S. Schubert, J.-M. Lehn, G. Baum, D. Fenske, *Angew. Chem.* **1997**, *109*, 1929; *Angew. Chem. Int. Ed. Engl.* **1997**, *36*, 1842; e) J. C. Jeffery, P. L. Jones, K. L. V. Mann, E. Psillakis, J. A. McCleverty, M. D. Ward, C. M. White, *Chem. Commun.* **1997**, 175; f) D. M. Bassani, J.-M. Lehn, K. Fromm, D. Fenske, *Angew. Chem.* **1998**, *110*, 2534; *Angew. Chem. Int. Ed.* **1998**, *37*, 2364; g) A. M. Garcia, F. J. Romero-Salguero, D. M. Bassani, J.-M. Lehn, G. Baum, D. Fenske, *Chem. Eur. J.* **1999**, *5*, 1803.

[7] P. N. W. Baxter, G. S. Hanan, J.-M. Lehn, *Chem. Commun.* **1996**, 2019.

[8] For recent examples of cages, see a) P. N. W. Baxter, J.-M. Lehn, G. Baum, D. Fenske, *Chem. Eur. J.* **1999**, *5*, 102; b) P. N. W. Baxter, J.-M. Lehn, B. O. Kneisel, G. Baum, D. Fenske, *Chem. Eur. J.* **1999**, *5*, 113; c) A. M. Garcia, D. M. Bassani, J.-M. Lehn, G. Baum, D. Fenske, *Chem. Eur. J.* **1999**, *5*, 1234; d) N. Takeda, K. Umemoto, K. Yamaguchi, M. Fujita, *Nature*, **1999**, *398*, 794; e) T. Kusukawa, M. Fujita, *J. Am. Chem. Soc.* **1999**, *121*, 1397; f) X. Sun, D. W. Johnson, D. L. Caulder, R. E. Powers, K. N. Raymond, E. H. Wong, *Angew. Chem.* **1999**, *111*, 1386; *Angew. Chem. Int. Ed.* **1999**, *38*, 1303; g) T. Beissel, R. E. Powers, T. N. Parac, K. N. Raymond, *J. Am. Chem. Soc.* **1999**, *121*, 4200.

[9] Circular helicates: a) D. P. Funeriu, J.-M. Lehn, G. Baum, D. Fenske, *Chem. Eur. J.* **1997**, *3*, 99; b) B. Hasenknopf, J.-M. Lehn, N. Boumediene, A. Dupont-Gervais, A. Van Dorsselaer, B. Kneisel, D. Fenske, *J. Am. Chem. Soc.* **1997**, *119*, 10956; for recent examples of rings, see: c) J. Manna, C. J. Kuehl, J. A. Whiteford, P. J. Stang, D. C. Muddiman, S. A. Hofstadler, R. D. Smith, *J. Am. Chem. Soc.* **1997**, *119*, 11611; d) J. Fan, J. A. Whiteford, B. Olenyuk, M. D. Levin, P. J. Stang, E. B. Fleischer, *J. Am. Chem. Soc.* **1999**, *121*, 2741; e) R.-D. Schnebeck, E. Freisinger, B. Lippert, *Chem. Commun.* **1999**, 675.

[10] M.-J. Blanco, M. Consuelo Jiménez, J.-C. Chambron, V. Heitz, M. Linke, J.-P. Sauvage, *Chem. Soc. Rev.* **1999**, *28*, 293.

[11] a) H. Sleiman, P. N. W. Baxter, J.-M. Lehn, K. Rissanen, *J. Chem. Soc. Chem. Commun.* **1995**, 715; b) P. N. W. Baxter, H. Sleiman, J.-M. Lehn, K. Rissanen, *Angew. Chem.* **1997**, *109*, 1350; *Angew. Chem. Int. Ed. Engl.* **1997**, *36*, 1294; c) H. Sleiman, P. N. W. Baxter, J.-M. Lehn, K. Rissanen, K. Aerola, *Inorg. Chem.* **1997**, *36*, 4734.

[12] a) J.-C. Chambron, C. O. Dietrich-Buchecker, J.-P. Sauvage in *Comprehensive Supramolecular Chemistry*, *Vol. 9* (Eds.: J. C. Atwood, J. E. D. Davies, D. D. MacNicol, F. Vögtle, J.-M. Lehn), Pergamon, Oxford, **1996**, pp. 43–83; b) M. Fujita, M. Aoyagi, F. Ibukuro, K. Ogura, K. Yamaguchi, *J. Am. Chem. Soc.* **1998**, *120*, 611; c) M. Fujita, *Acc. Chem. Res.* **1999**, *32*, 53.

[13] For a review on the preparation and properties of silver quantum dot superlattices, see: G. Markovich, C. P. Collier, S. E. Henrichs, F. Remacle, R. D. Levine, J. R. Heath, *Acc. Chem. Res.* **1999**, *32*, 415.

[14] Methods for the synthesis of 3, 3′-bipyridazines and their substituted derivatives have been reported; a) H. Igeta, T. Tsuchiya, M. Nakajima, H. Yokogawa, *Tetrahedron Lett.* **1969**, *28*, 2359; b) H. Igeta, T. Tsuchiya, M. Nakajima, C. Okuda, H. Yokogawa, *Chem. Pharm. Bull.* **1970**, *18*, 1228; c) H. Igeta, T. Tsuchiya, C. Okuda, H. Yokogawa, *Chem. Pharm. Bull.* **1970**, *18*, 1340; d) N. Biedermann, J. Sauer, *Tetrahedron Lett.* **1994**, *35*, 7935; d) H. Bleisinger, P. Scheidhauer, H. Dürr, V. Wintgens, P. Valat, J. Kossanyi, *J. Org. Chem.* **1998**, *63*, 990.

[15] For coupling procedures, see: a) Y. Yamamoto, Y. Azuma, H. Mitoh, *Synthesis*, **1986**, 564; b) M. Iyoda, H. Otsuka, K. Sato, M. Oda, *Bull. Chem. Soc. Jpn.* **1990**, *63*, 80; c) see ref. [14d] for the nickel-catalysed conversion of **4** to **5**.

[16] For another type of quadruply stranded helicate, see: D. A. McMorran, P. J. Steel, *Angew. Chem.* **1998**, *110*, 3495; *Angew. Chem. Int. Ed.* **1998**, *37*, 3295.

[17] Crystallographically characterised disilver complexes with short Ag^I–Ag^I bond lengths (2.8–2.9 Å) are relatively rare but have been described, see for example: a) M. Munakata, M. Maekawa, S. Kitagawa, M. Adachi, H. Masuda, *Inorg. Chim. Acta*, **1990**, *167*, 181; b) J. L. Coyle, V. McKee, J. Nelson, *Chem. Commun.* **1998**, 709.

[18] A. O. Orlov, I. Amlani, G. H. Bernstein, C. S. Lent, G. L. Snider, *Science* **1997**, *277*, 928.

[19] J.-M. Lehn, *Chem. Eur. J.* **1999**, *5*, 2455.

[20] G. V. Long, S. E. Boyd, M. M. Harding, I. E. Buys, T. W. Hambley, *J. Chem. Soc. Dalton Trans.* **1993**, 3175.

Received: June 19, 2000 [F2553]